

Martensitic transformation and shape memory effect in ferromagnetic Heusler alloy Ni_2FeGa

Z. H. Liu, M. Zhang, Y. T. Cui, Y. Q. Zhou, W. H. Wang, and G. H. Wu^{a)}

State Key Laboratory for Magnetism, Institute of Physics, Chinese Academy of Sciences, Beijing 100080, People's Republic of China

X. X. Zhang

Department of Physics, The Hong Kong University of Science and Technology, Clear Water Bay, Kowloon, Hong Kong, People's Republic of China

Gang Xiao

Department of Physics, Brown University, Providence, Rhode Island 02912

(Received 3 September 2002; accepted 11 November 2002)

We have synthesized ferromagnetic Heusler alloy Ni_2FeGa using the melt-spinning technique. The Ni_2FeGa ribbon, having a high chemical ordering $L2_1$ structure, exhibits a thermoelastic martensitic transformation from cubic to orthorhombic structure at 142 K and a premartensitic transformation. The alloy has a relatively high Curie temperature of 430 K, a magnetization of $73 \text{ Am}^2/\text{kg}$, and a low saturated field of 0.6 T. The textured samples with preferentially oriented grains show a completely recoverable two-way shape memory effect with a strain of 0.3% upon the thermoelastic martensitic transformation. © 2003 American Institute of Physics. [DOI: 10.1063/1.1534612]

Ferromagnetic shape memory alloys have attracted much attention due to their potential application as smart materials. Many such materials have been developed recently, such as Ni_2MnGa ,¹ Ni_2MnAl ,² Fe-Pd ,³ Co-Ni-Ga ,⁴ and Ni-Co-Al .⁵ Among them, Ni_2MnGa is the mostly studied alloy.⁶⁻⁸ Because of their application value, many groups are actively searching new magnetic shape memory alloys. In this letter, we report the fabrication of the ferromagnetic Heusler alloy Ni_2FeGa . While it is impossible to make this alloy using conventional methods, we have synthesized Ni_2FeGa ribbon by the melt-spinning technique. We will present its structure, magnetic properties, martensitic transformation, and shape memory.

We prepared the precursor ingot by melting pure metals in proportion in an induction furnace under the argon atmosphere. Subsequently the ingot was melted in a quartz tube and rapidly cooled by spinning onto a copper wheel, spinning at a linear velocity of about 25 m/s. We have analyzed the structure and microstructure using x-ray diffraction (XRD) and transmission electron microscopy (TEM). The standard four-probe technique was used to measure the temperature dependence of resistivity. We have measured ac magnetic susceptibility in an 77 Hz magnetic field of 5 Oe and over a temperature range of 77 to 450 K. We have also measured other magnetic properties using a superconducting quantum interference device magnetometer (Quantum Design MPMS).

The prepared spun ribbons are usually of a width of 6 mm and a thickness of $30 \mu\text{m}$. TEM observations along the relevant directions have identified that the Ni_2FeGa ribbon has cubic average structure with space group $Fm\bar{3}m$. Figure 1(a) shows a selected-area electron diffraction pattern along the $[001]$ -zone axis direction. All diffraction spots in this

pattern can be well indexed by a cubic cell with lattice parameter of $a = 5.70 \text{ \AA}$. Figure 1(b) shows the TEM observation along the free surface of a ribbon. This bright-field image reveals the typical texture microstructure of ribbons. The lamellar grains with the size of about $0.3 \times 0.5 \mu\text{m}^2$, crystallized under a fast-cooling condition, and formed longitudinally along the ribbon.

Figure 2 shows the powder XRD pattern for the Ni_2FeGa ribbon and precursor ingot at different temperatures. For the Ni_2FeGa ribbon, all intense peaks can be indexed to a cubic structure with calculated lattice parameters of $a = b = c = 5.7405 \text{ \AA}$ and $\alpha = \beta = \gamma = 90^\circ$, as shown in Fig. 2(b). The (111) superlattice reflection corresponding to the next-nearest-neighbor $L2_1$ ordering is observed. This is in agreement with a structural criteria for Heusler alloy used in the case of Ni_2MnAl .⁹ Figure 2(a) shows the diffraction pattern for the precursor ingot. The characteristic peaks reveal a γ solid solution phase with some embedded second phase of the composition of $\text{Ni}_{49}\text{Fe}_{32}\text{Ga}_{19}$.

XRD measurements have been performed at different temperatures to observe the structural evolution of the ribbon. As temperature is lowered to 80 K, new peaks, such as

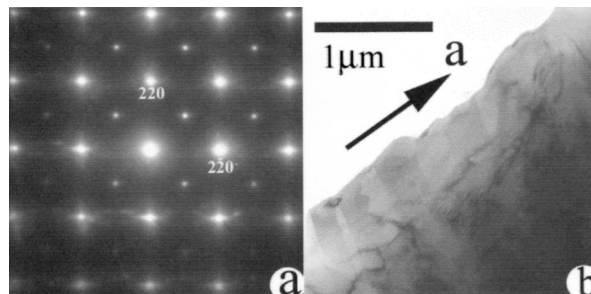


FIG. 1. Electron diffraction pattern along the $[001]$ -zone axis direction (a) and bright-field image of the investigated area along the free surface of a ribbon (b).

^{a)}Electronic mail: userm201@aphy.iphy.ac.cn

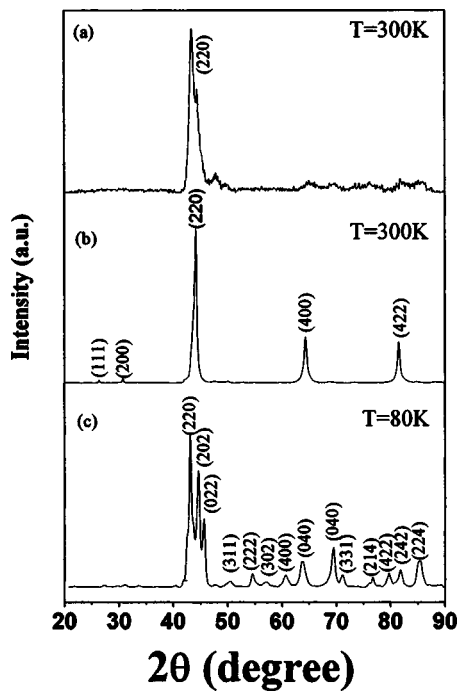


FIG. 2. XRD of the precursor ingot (a) at room temperature and melt-spun ribbon Ni_2FeGa taken at room temperature (b) and at 80 K (c).

(302) and (214), emerge. The original $(220)_{\text{cubic}}$ peak splits into $(220)_{\text{orth}}$, $(202)_{\text{orth}}$, and $(022)_{\text{orth}}$. The $(400)_{\text{cubic}}$ and $(422)_{\text{cubic}}$ peaks also have similar splitting behavior, as shown in Fig. 2(c). To index these characteristic peaks, we confirmed a cubic-to-orthorhombic (space group $Fmmm$) structural transition. The orthorhombic phase has lattice parameters: $a = 5.8565 \text{ \AA}$, $b = 5.7336 \text{ \AA}$, $c = 5.4507 \text{ \AA}$, and $\alpha = \beta = \gamma = 90^\circ$. These results clearly reflect a martensitic transformation during the cooling. Similar transformation has been seen in the well-known NiMnGa Heusler alloy.¹⁰

From the comparison between the structures of the ribbon and the precursor ingot, we can conclude that there exists a high chemical ordering structure $L2_1$, that is the Heusler alloy phase, in the Ni_2FeGa composition, similar to that found in Ni_2MnGa . For most Heusler alloys, the conventional synthesis is arc-melting followed by annealing at a specific temperature to achieve a structural transition from B2 to $L2_1$.¹¹ However, such a method failed in synthesizing Ni_2FeGa $L2_1$ structure. Our XRD and metallurgical examination revealed that a strong competition between forming γ solid solution phase and intermetallic phase during the conventional solidification process. Once the γ phase is formed, it would obstruct the formation of the pure $L2_1$ phase, even if a heat treatment was applied to the as-cast ingot. Our adoption of the melt-spinning ribbon technique impedes the formation of the γ phase, by enforcing a rapid cooling of the liquid state directly into the pure $L2_1$ phase. Thus, our method opens an avenue of searching for new Heusler alloys of interest.

Temperature dependence of the ac susceptibility of the Ni_2FeGa ribbon is shown in Fig. 3(a). It reveals a Curie temperature T_C of 430 K. Furthermore, there exist two first-order transitions, at 178 and 142 K, respectively, during cooling, and at 146 and 163 K during heating. Both transformations are thermoelastic. In contrast to the Ni_2FeGa ribbon,

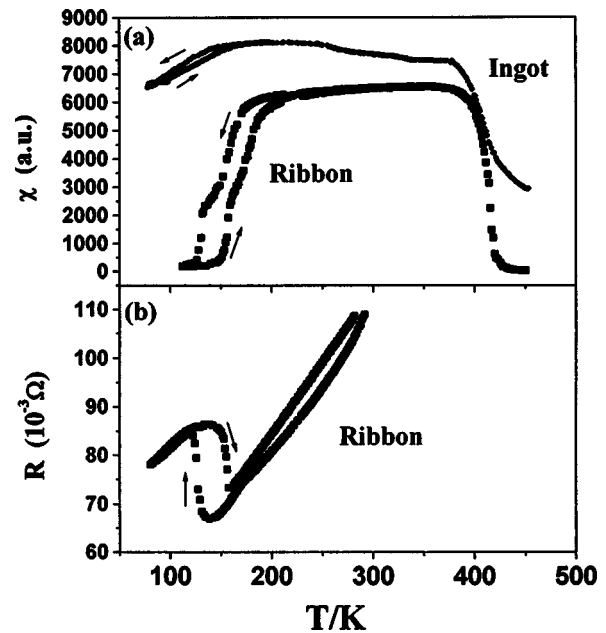


FIG. 3. Temperature dependence of ac magnetic susceptibility of Ni_2FeGa ribbon and ingot (a) and temperature dependence of electrical resistance of Ni_2FeGa ribbon (b).

the precursor ingot only shows weak and broad phase transitions both in first and second order, as shown in Fig. 3(a). The sharp first-order transformations and second-order magnetic transition in Ni_2FeGa ribbon are further evidences of the high chemical ordering structure in the melt-spun sample.

Figure 3(b) shows the temperature dependence of the resistance of the ribbon. There is one pronounced jump at the temperature corresponding to the transformation at 142 K in the susceptibility versus temperature curve during cooling. On the other hand, the XRD result also confirmed only one structural transition during cooling. Based on the well-known martensitic transformation behavior in Heusler alloy Ni_2MnGa ,¹² the transition at 142 K in the Ni_2FeGa ribbon can be identified as a martensitic transformation, while the one occurring at 178 K should be associated with the premartensitic transformation. The latter has been known as a consequence of the magnetoelastic interaction between the phonons and the magnons.¹³ The premartensitic transformation is evident in the ac susceptibility, but hidden in the measurement of x-ray, resistance, and magnetization at relatively large field.¹⁴

Figure 4 shows isothermal $M-H$ curves measured at the temperature above and below the martensitic transformation. Due to different magnetic anisotropies, the magnetization is hard to saturate below the martensitic transition, but easy to saturate above the transition. The martensite at lower temperature exhibits a high magnetization $73 \text{ Am}^2/\text{kg}$ and a high saturation field of 0.6 T, but decreasing to $60 \text{ Am}^2/\text{kg}$ and 0.15 T, respectively, for the parent phase at higher temperature. It should be noted that the martensite saturation field of 0.6 T in Ni_2FeGa is quite lower than that of about 1.0 T in Ni_2MnGa . A low saturation is preferred in applications.

The thermoelastic martensitic transformation observed in the Ni_2FeGa ribbon implies the existence of a shape memory effect. Figure 5 shows the strain as a function of temperature. Cooled from room temperature, the sample con-

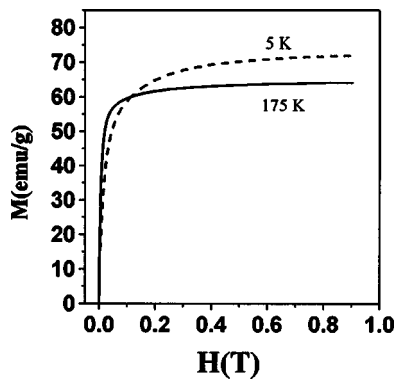


FIG. 4. Magnetization as a function of magnetic field above and below the martensitic transformation.

tracts about 0.3% upon the martensitic transformation. During heating and through the reverse martensitic transformation, the deformation is completely recovered by an expansion with the same value of 0.3%, showing a good two-way shape memory behavior in our unconstrained sample.

A spontaneous transformation strain, the two-way shape memory effect, is from the preferential orientation of martensitic variants upon the transformation. In Ni_2MnGa , a large two-way shape memory was usually obtained in single crystalline or prestressed samples. However, a large strain up to 0.3% has been observed in our Ni_2FeGa melt-spun ribbon,

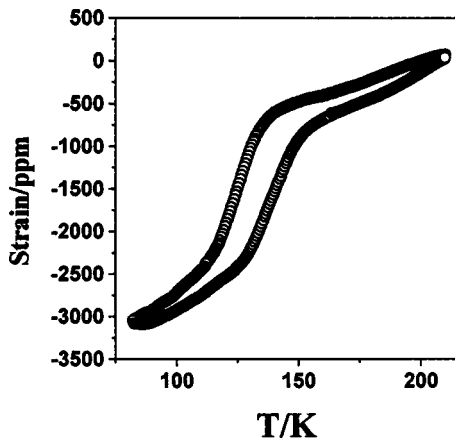


FIG. 5. Strain as a function of temperature measured in the ribbon direction.

which is composed of many small-sized polycrystalline-textured lamellar grains. This implies that the internal stress as a result of melt-spinning plays an important role in orienting the variants.

In conclusion, we have synthesized ferromagnetic Heusler alloy of Ni_2FeGa by using the melt-spinning technique. The Ni_2FeGa ribbon has a pure cubic $L2_1$ structure and shows a thermoelastic martensitic transformation from cubic to orthorhombic structure at 142 K. The Ni_2FeGa ribbon has a Curie temperature of 430 K, a saturated magnetization of $73 \text{ Am}^2/\text{kg}$, and a low saturated field of 0.6 T. We have obtained a two-way shape memory effect with a completely recoverable strain of 0.3% upon the thermoelastic martensitic transformation. The Ni_2FeGa alloy with its large shape deformation and a low saturated field of 0.6 T, about half of that of Ni_2MnGa , renders it a good candidate for applications.

This work was supported by State Key Project of Fundamental Research Grant, National Natural Science Foundation of China Grant No. 50131010, and Hong Kong RGC grant (HKUST6059/02E).

- ¹P. J. Webster, K. R. A. Ziebeck, S. L. Town, and M. S. Peak, *Philos. Mag. B* **49**, 295 (1984).
- ²A. Fujita, K. Fukamichi, F. Gejima, R. Kainuma, and K. Isshida, *Appl. Phys. Lett.* **77**, 3054 (2001).
- ³Y. Furuya, N. W. Hagood, H. Kimura, and T. Watanabe, *Mater. Trans., JIM* **39**, 1248 (1998).
- ⁴M. Wuttig, J. Li, and C. Craciunescu, *Scr. Mater.* **44**, 2393 (2001).
- ⁵K. Oikawa, L. Wulff, T. Iijima, F. Gejima, T. Ohmori, A. Fujita, K. Fukamichi, R. Kainuma, and K. Isshida, *Appl. Phys. Lett.* **79**, 3290 (2001).
- ⁶K. Ullakko, J. K. Huang, C. Kantner, R. C. O'Handley, and V. V. Kokorin, *Appl. Phys. Lett.* **69**, 1966 (1996).
- ⁷R. D. James and M. Wuttig, *Philos. Mag. A* **77**, 1273 (1998).
- ⁸G. H. Wu, C. H. Yu, L. Q. Meng, J. L. Chen, F. M. Yang, S. R. Qi, W. S. Zhan, Z. Wang, Y. F. Zheng, and L. C. Zhao, *Appl. Phys. Lett.* **75**, 2990 (1999).
- ⁹Y. Sutou, I. Ohnuma, R. Kainuma, and K. Ishida, *Metall. Mater. Trans. A* **29**, 2225 (1998).
- ¹⁰Y. Ma, S. Awaji, K. Watanabe, M. Matsumoto, and N. Kobayashi, *Solid State Commun.* **113**, 671 (2000).
- ¹¹V. V. Khovailo, T. Takagi, A. N. Vasilev, H. Miki, M. Matsumoto, and R. Kainuma, *Phys. Status Solidi A* **183**, R1 (2001).
- ¹²W. H. Wang, J. L. Chen, S. X. Gao, G. H. Wu, Z. Wang, Y. F. Zheng, L. C. Zhao, and W. S. Zhan, *J. Phys.: Condens. Matter* **13**, 2607 (2001).
- ¹³A. Planes, E. Obrado, A. Gonzalez-comas, and L. Manosa, *Phys. Rev. Lett.* **79**, 3926 (1997).
- ¹⁴F. Zuo, X. Su, P. Zhang, G. C. Alexandrakakis, F. Yang, and K. H. Wu, *J. Phys.: Condens. Matter* **13**, 2607 (2001).